Turkish Journal of Electrical Engineering & Computer Sciences

http://journals.tubitak.gov.tr/elektrik/

Research Article

Turk J Elec Eng & Comp Sci
(2016) 24: 605 – 620

doi:10.3906/elk-1309-137

Chattering-eliminated adaptive sliding-mode control: an experimental comparison study

Murat FURAT*, **İlyas EKER**
Department of Electrical and Electronics Engineering, Faculty of Engineering and Architecture,
Çukurova University, Adana, Turkey

Received: 17.09.2013 • **Accepted/Published Online:** 23.12.2013 • **Final Version:** 05.02.2016

Abstract: The present paper deals with a new adaptive sliding-mode control. The switching and equivalent control laws include adaptive gains. An error-dependent adaptive gain in the switching control law and an adaptive parameter in the equivalent control law with respect to open-loop transient response of the system are proposed to eliminate chattering and to increase the performance of the controller. The proposed approach results in chattering elimination without using any complex calculation-based methods, which is highly useful for practical applications. The number of independent gains is also minimized. Therefore, tuning of those gains is simplified. The proposed controller is compared experimentally using an electromechanical system with five different conventional sliding-mode controllers presented in the literature. The experimental results are presented to show the effectiveness of the proposed controller particularly regarding the accuracy of control input, disturbance rejection, and being an alternative controller to use in industrial applications.

Key words: Sliding-mode control, chattering elimination, adaptive gain

1. Introduction

Sliding-mode control (SMC) was presented by Utkin in 1977 in the international literature that was previously developed in Russia [1]. The method has several advantages such as low sensitivity to system parameter variations and robustness against external disturbances. Furthermore, the solution algorithm of the method provides a systematic design procedure with reduction of the requirements of the exact system model [2]. The method has been extensively studied and implemented for both linear and nonlinear systems, multiinput/multioutput systems, and discrete-time and large-scale systems [2–5].

In SMC, the control strategy is determined by the sum of two control laws: switching and equivalent control laws [1]. The switching control law enforces the system states to the predetermined sliding surface in a finite time. When the sliding-mode occurs, the closed-loop system becomes insensitive to parameter variations and robust to matched disturbances by means of the equivalent control law derived from the sliding function [6].

The switching control signal switches from one value to another infinitely fast in an ideal SMC. Therefore, the high frequency switching signal produces undesired oscillations in the control signal, called chattering, due to the presence of unmodeled dynamics of the system. Because of the limitations of physical systems such as time lag, transportation lag, time delay, and dead time, it is not possible to achieve such switching control by real actuators as demanded by the theory of SMC [2–5,7,8]. This phenomenon is the main drawback of

*Correspondence: mfurat@cu.edu.tr

the conventional SMC, and it results in low control accuracy and is harmful for the moving parts of the real actuators depending on the magnitude of the oscillation. A detailed analysis of chattering types with their reasons was given in [9]. In the literature, the proposed switching control laws having constant switching gain were still capable of producing chattering [6,7,10,11]. There are many individual studies in the literature to alleviate chattering [2–5,12]. On the other hand, a reasonable magnitude of oscillation may be acceptable in the control signal that rejects the disturbances.

The systematic design procedure of the conventional SMC, called the equivalent approach, was introduced in [1]. The equivalent signal is obtained by equating the first-time derivative of the sliding surface function to zero. The resulting algebraic system is then solved for the equivalent control signal. If the equivalent control exists, it is substituted into the sliding surface to find the ideal sliding mode [1]. In the literature, a variety of sliding functions were proposed, i.e. a PI-PD sliding surface [6], an integral augmented sliding surface [7], a PID sliding surface [10], and an integral-differential sliding surface acting on the tracking error [11]. A different sliding function was developed based on the internal model of the processes having a time constant greater than the dead-time of the process [13]. In addition, soft computing methods, such as fuzzy logic, neural networks, and the genetic algorithm, have been also integrated to enhance the SMC performance by using high-speed computers. The state of the art of SMC with soft computing methods was well examined in [14,15].

Remark 1 The developments in computer technology have facilitated the design and modification of controllers with fast computation in the recent decades. The control signal is produced at each sampling period with respect to the controller. However, the sampling period was only rarely taken into account [16,17].

Remark 2 The number of independent controller parameters increases the difficulty in tuning, e.g., there are two parameters to be tuned in [1], three parameters in [11], four parameters in [7], five parameters in [10], and six parameters in [6]. Soft computing methods were proposed in some works that require expert knowledge of both the controller and the system by the user [14,15,17–19].

The first aim of the present paper is to propose an adaptive sliding-mode controller for uncertain real systems that provides fast convergence in the reaching phase, produces no chattering in the sliding mode, and has good tracking performance in both the transient state and steady state. The contribution appears at two points: a new guideline to obtain the adaptive parameter in the equivalent control law, and a new adaptive gain in the switching control law. The adaptive parameter in the equivalent control law depends on the sampling period and the open-loop output characteristics of the system at maximum possible input. The switching control gain changes adaptively with respect to the magnitude of the tracking error in order to limit the boundary of switching control magnitude dynamically.

The second aim is to present how much the performance of the proposed controller is superior to the other conventional algorithms by means of graphical and numerical results of the experiments carried on an electromechanical system. For this purpose, five different conventional algorithms were selected from the literature.

The organization of the present paper is as follows. The design principles of the proposed controller are explained in Section 2. In Section 3, the electromechanical system is presented. The experimental evaluation and comparison of the proposed controller with the other sliding-mode controllers given in the literature are given in Section 4. The discussion of the experimental results is given in the next section. Finally, concluding remarks are provided in the last section.

2. Proposed sliding-mode control

The first step is to evaluate the equivalent control law, $u_{eq}(t)$, which is obtained by solving the first-time derivative of the sliding function, $\dot{\sigma}(t) = 0$ [6,7,10,11], and the second step is to design the switching control law, $u_{sw}(t)$. The control input is then found as:

$$u(t) = u_{eq}(t) + u_{sw}(t). \tag{1}$$

Since simplicity is desired for a controller, the sliding surface in [1] is considered for the second-order system as:

$$\sigma(t) = \lambda e(t) + \dot{e}(t), \tag{2}$$

where $e(t)$ is the tracking error and λ is an independent positive constant, $\lambda \in R^+$.

In the digital implementation, $\dot{e}$ is approximated as [17,20]:

$$\dot{e} \approx \frac{e[k] - e[k-1]}{t_s}, \tag{3}$$

where $e[k]$ is the tracking error at the kth sample and t_s is the sampling period.

Since current computer technology allows us to compute control signals in small sampling periods, the magnitude of the sliding function computed at each sampling period is determined by the dominant term, $\dot{e}(t)$, when the direct differentiation of Eq. (3) is used. Decreasing the sampling period increases the effects of $\dot{e}(t)$ on the magnitude of the sliding function. It seems that the constant λ should be increased to solve this issue. However, such an approach increases the variations of the sliding function in magnitude, which results in undesired oscillatory control signal, so-called chattering. The other solution, decreasing the magnitude of the dominant term with an adaptive parameter, proportional to $\lambda e(t)$, should then be considered as:

$$\sigma(t) = \lambda e(t) + \beta \dot{e}(t), \tag{4}$$

where β is a positive adaptive parameter obtained from the open-loop characteristics of the system.

Taking the first-time derivative of the sliding function given in Eq. (4), one has:

$$\dot{\sigma}(t) = \lambda \dot{e}(t) + \beta \ddot{e}(t), \tag{5}$$

where $\ddot{e}(t) = \ddot{r}(t) - \ddot{y}(t)$, $r(t)$ is the set point, and $y(t)$ is the system output.

Substituting $\ddot{e}(t)$ into Eq. (5), one has:

$$\dot{\sigma}(t) = \lambda \dot{e}(t) + \beta \left(\ddot{r}(t) - \ddot{y}(t)\right). \tag{6}$$

A second-order, linear, time-invariant uncontrolled system is considered as:

$$\ddot{y}(t) = -A\dot{y}(t) - By(t) + Cu(t) + D(t), \tag{7}$$

where $D(t)$ represents unmodeled system dynamics, external load disturbance, and other uncertainties and is bounded with $|D(t)| < D_{\max}$, $D_{\max} \in R^+$. A, B, and C are known nominal plant parameters.

Substituting Eq. (7) into Eq. (6) yields:

$$\dot{\sigma}(t) = \lambda \dot{e}(t) + \beta \left(\ddot{r}(t) + A\dot{y}(t) + By(t)\right) - \beta Cu(t) - \beta D(t). \tag{8}$$

The equivalent control law is obtained from nominal system parameters, i.e. $D(t)=0$, when $\dot{\sigma}(t)=0$:

$$u_{eq}(t)=\frac{1}{C}\left[\frac{\lambda}{\beta}\dot{e}(t)+\ddot{r}(t)+A\dot{y}(t)+By(t)\right]. \tag{9}$$

The equivalent control with the uncertainty is given as:

$$\hat{u}_{eq}(t)=u_{eq}(t)+C^{-1}D(t). \tag{10}$$

Since the control input is the sum of the equivalent and switching control laws, as given in Eq. (1), the ideal sliding mode is obtained by substituting the control input into Eq. (8) [1]. Thus, we have the following.

$$\begin{aligned}\dot{\sigma}(t) &= \lambda\dot{e}(t)+\beta\left(\ddot{r}(t)+A\dot{y}(t)+By(t)\right)-\beta C\left\{u_{eq}(t)+u_{sw}(t)\right\}-\beta D(t)\\ &= \lambda\dot{e}(t)+\beta\left(\ddot{r}(t)+A\dot{y}(t)+By(t)\right)\\ &\quad -\beta C\left\{\tfrac{1}{C}\left[\tfrac{\lambda}{\beta}\dot{e}(t)+\ddot{r}(t)+A\dot{y}(t)+By(t)\right]+u_{sw}(t)\right\}-\beta D(t)\end{aligned} \tag{11}$$

After simplifications, one has:

$$\dot{\sigma}(t)=-\beta C u_{sw}(t)-\beta D(t). \tag{12}$$

Remark 3 In the transient state, the large switching gain provides faster convergence to the desired point. On the other hand, the selected large gain causes chattering in the steady state. The smaller gain results in slower convergence in the transient state with small or no chattering in the steady state.

It is obvious that the constant gain in the switching control law, even if it is used with a smooth function, causes a chattering/tracking performance dilemma. Therefore, a new adaptive rule should be considered for the switching control so that it has large magnitude in the transient state and small magnitude in the steady state [21]. For this purpose, a new switching signal is proposed as follows:

$$u_{sw}(t)=\begin{cases} k_s r^2(t)\tilde{e}(t)sgn\left(k_{sf}\frac{\sigma(t)}{\tilde{e}(t)}\right) & \text{if } k_s r^2(t)\tilde{e}(t)sgn\left(k_{sf}\frac{\sigma(t)}{\tilde{e}(t)}\right)<U_{\max} \\ U_{\max} & \text{otherwise}\end{cases}, \tag{13}$$

where k_s, k_{sf} are the positive constants. $U_{\max}$ is maximum control input, $k_s, k_{sf}, \varepsilon \in R^+$, k_s is switching gain, k_{sf} is a smoothing factor, $\tilde{e}(t)=|e(t)|+\varepsilon$, and ε is a small number used to avoid issues with division by zero.

2.1. Obtaining the adaptive parameter, β

In the proposed controller, the adaptive parameter, β, is determined by using the sampling period and the open-loop step response of the system when the maximum permissible step input is applied. In the proposed sliding function, there are two parameters in the sliding surface, λ and β, that play a role in converging the sliding function to the desired equilibrium point, $\sigma(t)=0$. The parameter, β, is determined by using the open-loop characteristics of the system. In Figure 1, a line is drawn on the transient region of the output having the most linear variations. The coordinates of a selected point on the line are used to determine the slope of the line, α. If the time delay of the system in Figure 1 is too small, it can be omitted when obtaining the slope. Since the equilibrium point is $\sigma(t)=0$, the sliding function is equated to zero:

$$\sigma(t)=\lambda e(t)+\beta\dot{e}(t)=0. \tag{14}$$

In Eq. (14), the dominant term of the sliding surface function is $\beta\dot{e}(t)$ as considering Eq. (5). The magnitude of $\dot{e}(t)$ increases when the sampling period decreases. The resulting unnecessary oscillation can be minimized by decreasing β. Thus, β is introduced as a function of set point, sampling period, and the slope of the line drawn on the maximum region of the output as follows:

$$\beta\left(r(t), t_s\right) = \frac{\alpha t_s}{r(t)}\lambda, \tag{15}$$

where α is the slope of the linear line illustrated in Figure 1, $\alpha = (y_2 - y_1)/(t_2 - t_1)$, $r(t)$ is the set point, and t_s is the sampling period. $r(t)$ does not change significantly and is assumed to be constant for simplification.

The proposed sliding function has minimum magnitude that minimizes the unnecessary oscillations in the switching control at each sampling period. The relation, given in Eq. (15), reduces the parameter number by one and minimizes the variations in $\sigma(t)$.

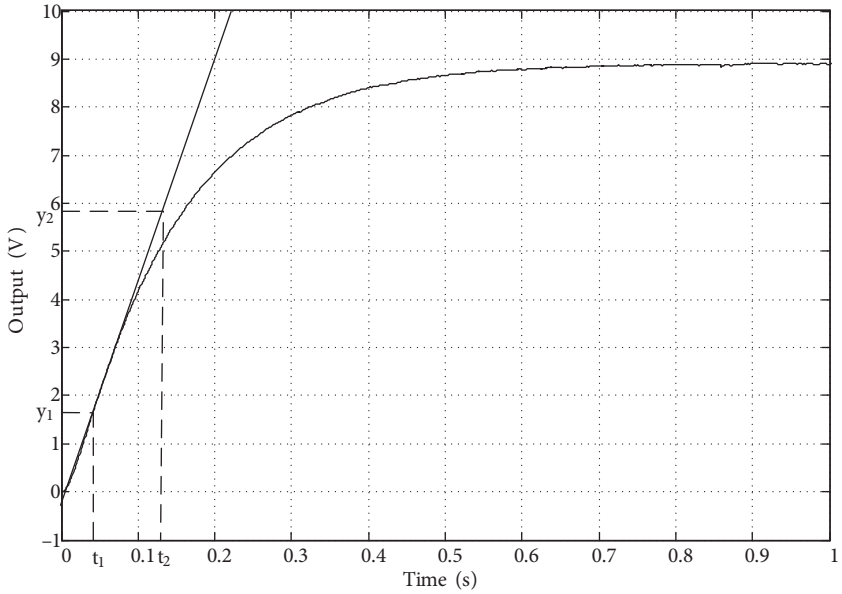

Figure 1. Open-loop output characteristics of a second-order system.

2.2. Effect of switching control gain parameters

The term $\tilde{e}(t)$ in Eq. (13) has large magnitude in the transient state, which is required for faster convergence, and it has small magnitude in the steady state, which reduces or eliminates the chattering. The switching control always acts on the closed-loop system because of the error caused by the parametric perturbations and uncertainties even if its magnitude converges to zero [21]. The square of the set point value produces the required switching signal magnitude exponentially for faster convergence of system states in the transient state. The maximum gain of the switching control is limited by k_s assuming that $r(t) \neq 0$ is a set point. The magnitude of $r^2(t)\tilde{e}(t)$ is much larger than the set point initially. Thus, in practical cases, it can be tuned starting from small values and increased boundlessly with small steps observing the performance of the closed-loop system.

2.3. Stability of the proposed controller

The stability of the proposed algorithm is investigated using the Lyapunov stability theorem. The selected Lyapunov function is as follows:

$$V(t) = \frac{1}{2}\sigma^2(t). \tag{16}$$

The first-time derivative of the selected Lyapunov function is obtained as:

$$\begin{aligned} \dot{V}(t) &= \sigma(t)\dot{\sigma}(t) \\ &= \sigma(t)\left(-\beta C k_s r^2(t)\tilde{e}(t) sgn\left(k_{sf}\frac{\sigma(t)}{\tilde{e}(t)}\right) - \beta D(t)\right) \end{aligned}. \tag{17}$$

Since $sgn\left(k_{sf}\frac{\sigma(t)}{\tilde{e}(t)}\right) = \frac{|\sigma(t)|}{\sigma(t)}$, the derivative of Lyapunov function becomes:

$$\begin{aligned} \dot{V}(t) &= \sigma\left(-\beta k_s C r^2(t)\tilde{e}(t)\frac{|\sigma(t)|}{\sigma(t)} - \beta D(t)\right) \\ &= -\beta k_s C r^2(t)\tilde{e}(t)\,|\sigma(t)| - \beta\sigma(t)D(t) \\ &\leq -\beta k_s C r^2(t)\tilde{e}(t)\,|\sigma(t)| + \beta\,|\sigma(t)|\,D_{\max} \\ &= -\,|\sigma(t)|\left(\beta k_s C r^2(t)\tilde{e}(t) - \beta D_{\max}\right) \\ &< 0. \end{aligned} \tag{18}$$

Here, $D_{\max} > |D(t)|$. If the requirement $k_s > \frac{D_{\max}}{Cr^2(t)\tilde{e}(t)}$ is satisfied then the stability of the proposed controller is guaranteed in the sense of the Lyapunov stability theorem.

The well-known reason for the chattering is the signum function used in switching control. Thus, the smooth function, tangent hyperbolic, is preferred as follows:

$$u_{sw}(t) = \begin{cases} k_s r^2(t)\tilde{e}(t)\tanh\left(k_{sf}\frac{\sigma(t)}{\tilde{e}(t)}\right) & \text{if } k_s r^2(t)\tilde{e}(t)\tanh\left(k_{sf}\frac{\sigma(t)}{\tilde{e}(t)}\right) < U_{\max} \\ U_{\max} & \text{otherwise} \end{cases}. \tag{19}$$

3. Description of the electromechanical system

The electromechanical system consists of a DC motor and a tachogenerator directly connected to the shaft of the motor, which is used to obtain the feedback signal as illustrated in Figure 2. The specifications of the motor are given in Table 1.

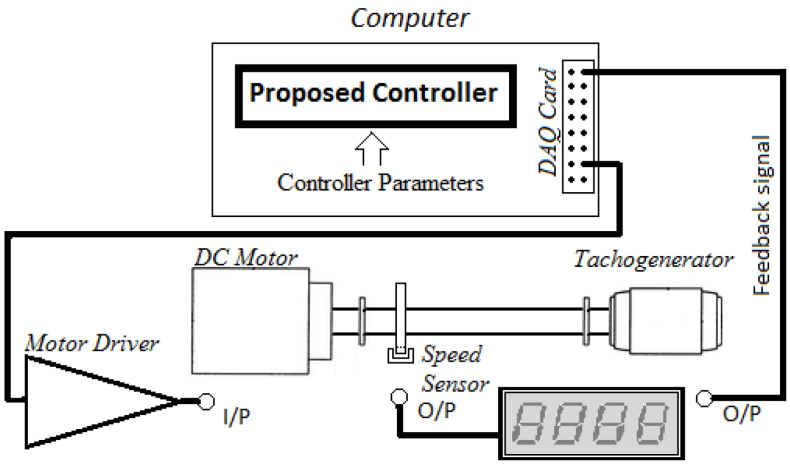

Figure 2. Block diagram of the experimental system.

Table 1. DC motor specifications.

Armature resistance	6.2 Ω
Stall current	1.93 A
Starting torque	7 Ncm/A
Torque constant	3.5 Ncm/A
Efficiency	70%–80%
Shaft speed at no load	2400 rpm (max)

The voltage induced at the terminals of the tachogenerator is proportional to the shaft speed. The tachogenerator produces output of magnitude 2.37 V at 600 rpm, 4.48 V at 1200 rpm, and 6.71 V at 1800 rpm shaft speed. The controller is designed with a computer and the produced control signal is applied to the motor via a DAQ and a motor driver. The output of the DAQ is limited by ± 10 V and the control signals are cropped at the limit. The closed-loop experiments were performed with 5 ms sampling time.

4. Experimental application and results

The nominal system parameters given in Eq. (9), A, B, and C, are obtained using the first-order plus dead-time method [22]. A step input of magnitude 5.12 V is applied to the armature of the motor. The output of the tachogenerator is measured. Using the output data, the system parameters are found to be $K = 0.86$, $T = 0.145$, $L = 0.0035$, $A = 292.61$, $B = 1970.40$, and $C = 1694.58$. The modeling error (real system output – model output) is between +30 rpm and –18 rpm speed deviations corresponding to 4% of the output including transient-state and steady-state outputs as illustrated in Figure 3.

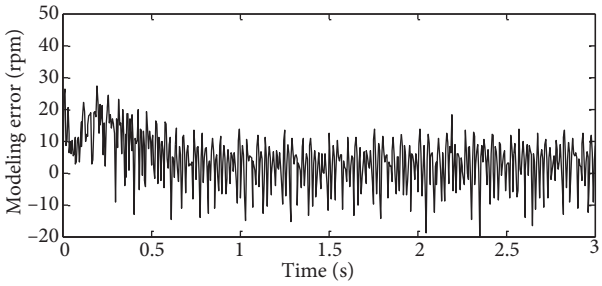

Figure 3. Modeling error of the real system.

The controller parameters were tuned so that minimum rise time, settling time, and delay time were as desired without overshoot at the output.

The experimental applications are divided into two sections. In the first section, the chattering elimination of the proposed switching control is presented. In the second section, five different conventional sliding-mode controllers are compared with the proposed controller. The experimental results are given graphically and statistically.

4.1. Chattering elimination with the proposed switching control

In the theory of conventional sliding mode, the switching control changes infinitely fast from one value to another, producing chattering in the control signal provided by the signum function in the switching control. The chattering effect of such switching control was experimentally tested with the proposed sliding function

where $\lambda = 14$ and $\beta = 0.6667$ were selected for the sliding function parameters and the switching gain was selected as 3.3. The resulting chattering signal at 1200 rpm shaft speed is shown in Figure 4.

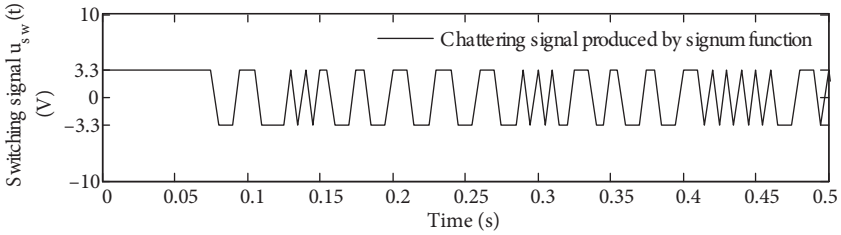

Figure 4. The chattering signal with signum function.

Instead of using the signum function with constant gain, the proposed switching control was used to reduce chattering in the control signal. In Figure 5, the resulting switching signal at 1200 rpm shaft speed is illustrated, where λ and β were kept the same and $k_s = 0.45$ and $k_{sf} = 0.18$ were selected for the proposed switching control so that nearly the same rise time at the output was obtained when both switching controls were used.

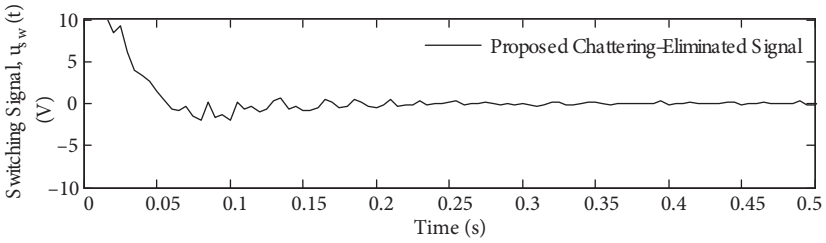

Figure 5. Chattering elimination with the proposed switching control.

Square wave command tracking responses of both switching controls were also investigated by applying 1200 $\pm$ 100 rpm shaft speeds. The corresponding control signals are shown in Figure 6. From Figures 4–6, it is evident that the chattering was significantly eliminated with the proposed switching control law as compared with Eq. (2).

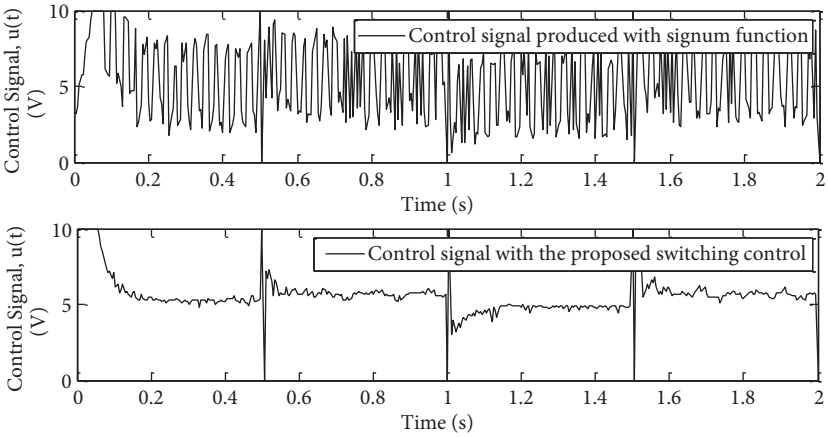

Figure 6. Chattering elimination with the proposed switching control for 1200 $\pm$ 100 rpm command tracking.

The variations of the adaptive gain, $k_s r^2(t)\tilde{e}(t)$, in the proposed switching control law are shown in Figure 7. The magnitude of the proposed switching control changes with respect to the magnitude of the error. When the set point is changed, its magnitude increases in the transient state and converges to zero in the steady state.

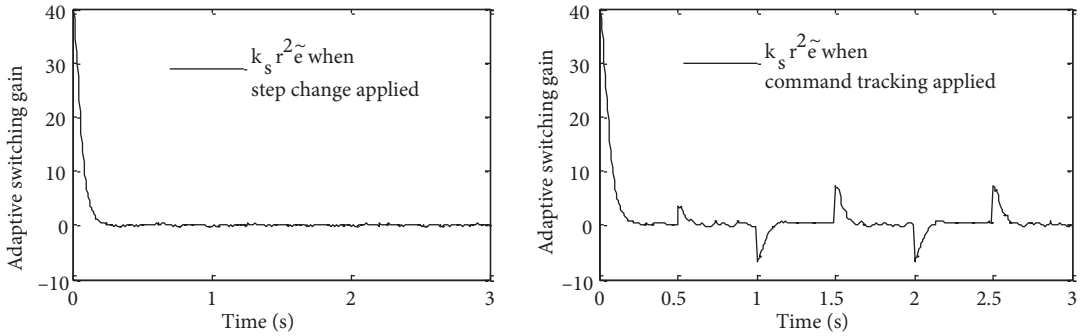

Figure 7. Change of adaptive switching control gain when step change and command tracking are applied.

4.2. Comparison experiments

The proposed controller was applied to the motor to evaluate the closed-loop performance and to compare the controllers selected from the literature. The control inputs of the controllers are given in Table 2.

Table 2. Experimentally evaluated controllers with the control laws.

Conventional sliding-mode controllers	Control inputs
Variable structure systems with sliding modes [1]	$u_{eq}(t) = \frac{1}{C}\left(\ddot{r}(t) + (A-\lambda)\dot{y}(t) + By(t) + \lambda\dot{r}(t) - \lambda\dot{y}(t)\right)$ $u_{sw}(t) = ksgn(\sigma(t))$
Sliding mode control: an approach to regulate nonlinear chemical processes [11]	$u_{eq}(t) = \frac{\tau t_0}{K}\left[\frac{1}{\tau t_0}y(t) + \lambda_0 e(t)\right]$ $u_{sw}(t) = K_D \frac{\sigma(t)}{\lvert\sigma(t)+\delta_D\rvert}$
Sliding mode control with PID sliding surface [10]	$u_{eq}(t) = \frac{1}{k_d C}\left[k_p\dot{e}(t) + k_i e(t) + k_d\ddot{r}(t) + k_d A\dot{y}(t) + k_d By(t)\right]$ $u_{sw}(t) = k_{sw}\text{sat}\left(\sigma(t)/\Omega\right)$
Sliding mode control of stable systems [6]	$u_{eq}(t) = \frac{TL}{k_4 K}\left[\left(\frac{k_4}{TL} - k_2\right)y(t) + k_2 r(t)\right]$ $u_{sw}(t) = k_d \tanh\left(\sigma(t)/\delta_d\right)$
Sliding mode control with integral augmented sliding surface [7]	$u_{eq}(t) = \frac{1}{C}[\ddot{r}(t) + (A-\lambda)\dot{y}(t) + (B+k_i)y(t) + \lambda\dot{r}(t) + k_i r(t)]$ $u_{sw}(t) = \kappa \tanh\left(\sigma(t)/\phi\right)$

All the controllers showed the best performance with the selected appropriate parameters tabulated in Table 3. The step responses of the experimental application to the set point change of magnitude 4.48 V corresponding to 1200 rpm shaft speed are illustrated in Figure 8. Time-domain step response specifications of the closed-loop system are given in Table 4 for comparison. The controller presented in [1] has maximum rise time and settling time while the minimum of them was measured from the controller from [11]. The

delay time, that is the time to reach the output to 50% of set point, was obtained as maximum from the controller from [1]. The minimum delay time was observed from [11], followed by the controller from [7] and the proposed one. The minimum output speed deviation means that the produced control input best matches the uncertainties, disturbances, and measurement noises. Among the controllers, the minimum output speed deviations were observed when using the proposed controller. Meanwhile, the transient-state performance of [11] is quite acceptable without considering output speed deviation in the steady state.

Table 3. Parameters of the experimentally evaluated controllers.

Conventional sliding-mode controllers	Parameters
Variable structure systems with sliding modes [1]	$\lambda = 13.75$, $k = 1.5$
Sliding mode control: an approach to regulate nonlinear chemical processes [11]	$\lambda_0 = 3600$, $K_D = 5.2$, $\delta_D = 3$
Sliding mode control with PID sliding surface [10]	$k_p = 30$, $k_i = 1$, $k_d = 1.1$, $k_{sw} = 5.2$, $\Omega = 20$
Sliding mode control of stable systems [6]	$k_1 = 19.5$, $k_2 = 100$, $k_3 = 9.76$, $k_4 = 0.1$, $k_d = 3.5$, $\delta_d = 20$

Table 4. Time-domain step response specifications of the controllers.

Conventional sliding-mode controllers	Rise time (ms)	Settling time (ms)	Output speed deviation (±rpm)	Delay time (ms)
Variable structure systems with sliding modes [1]	178	225	36	145
Sliding mode control: an approach to regulate nonlinear chemical processes [11]	91	120	21	50
Sliding mode control with PID sliding surface [10]	100	160	27	80
Sliding mode control of stable systems [6]	135	165	24	75
Sliding mode control with integral augmented sliding surface [7]	160	210	21	60
Proposed controller	99	147	7	65

In Figure 8, the maximum delay time was clearly seen for the output of [1]. The controllers from [7,11] produced smaller variations in magnitude as compared to the others [1,6,10] and the proposed controller.

The control signals produced by the controllers are shown in Figure 9. It is obvious that the controllers in [1,10] produced chattering. However, the other controllers [6,7,11] and the proposed one produced smoother signals than those of [1,10]. The control signals produced by [10,11] and the proposed controller exceeded the limit of DAQ (± 10 V) in the transient state.

The main object of the SMC is to force the system trajectory to zero, $e(t) = \dot{e}(t) = 0$, the desired value, and to keep them at that point. In Figure 10, the errors versus its first-time derivative for the proposed controller is illustrated.

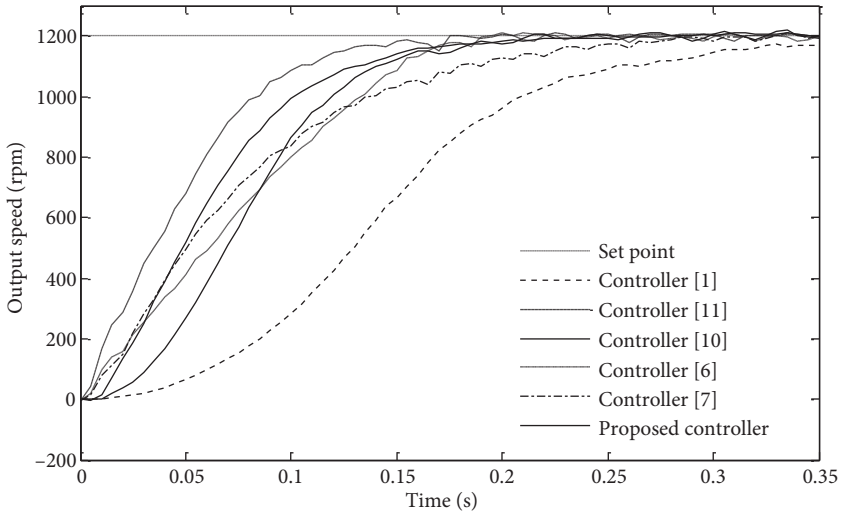

Figure 8. Transient states of the step responses.

Since the defined sliding functions of the controllers are based on the error and its first-time derivative, it is expected that the sliding function also converges to the equilibrium point, $\sigma(t) = 0$. The sliding functions of the controllers versus time are illustrated in Figure 11. Among the controllers, the magnitude of the sliding function of the controller in [11] converges to a value different than zero and is nearly stable at that value, as already stated in [11]. This is the main drawback of the controller from [11] when considering long-time application to uncertain real systems. It is difficult to stabilize the sliding function around any value for a long time under uncertain conditions.

In the literature, several performance indices tabulated in Table 5 were used to measure the performances of the controllers [23,24]. The operating point is 1200 rpm shaft speed and all the controllers' parameters in Table 3 were used. The tracking performances of the controllers were measured for the shaft speeds of 600, 1200, and 1800 rpm. The performance indices were calculated using the voltage-based output error for closed-loop experiments for a duration of 3 s.

The tracking accuracy is related to the produced control input accuracy. As the set point speed increased, the minimum absolute error (IAE) measured at the output was obtained from the proposed controller. The measured IAE values when using the controllers in [1,11] were relatively higher than those of other controllers. In addition, at higher speeds over the operating point, the minimum ISE was obtained from the proposed controller, which means that when the speed increases, the proposed controller produces a more accurate control signal than the other controllers. On the other hand, the ISCI index of the proposed controller was measured to be minimum while the error-based indices were higher than those of the other controllers at low speed. This may be due to the matching capacity of the proposed controller at low speeds, with increased friction and load. The present case could be eliminated by changing the control parameters. It can be seen using Table 5 that the matching capabilities of the methods seem different at different speeds.

The ISCI criterion indicates how much power is consumed by the controller. At all speeds, nearly the same amount of power was consumed by the controllers.

The robustness of the controllers to an external load disturbance is measured with a step-periodic signal of magnitude ± 0.37 V, corresponding to ± 100 rpm shaft speed, added to the measured output. The output responses of the evaluated controllers and the proposed one are illustrated in Figure 11. The controllers in [6,7] and the proposed one are capable of recovering the external load disturbance completely. The controller in [10]

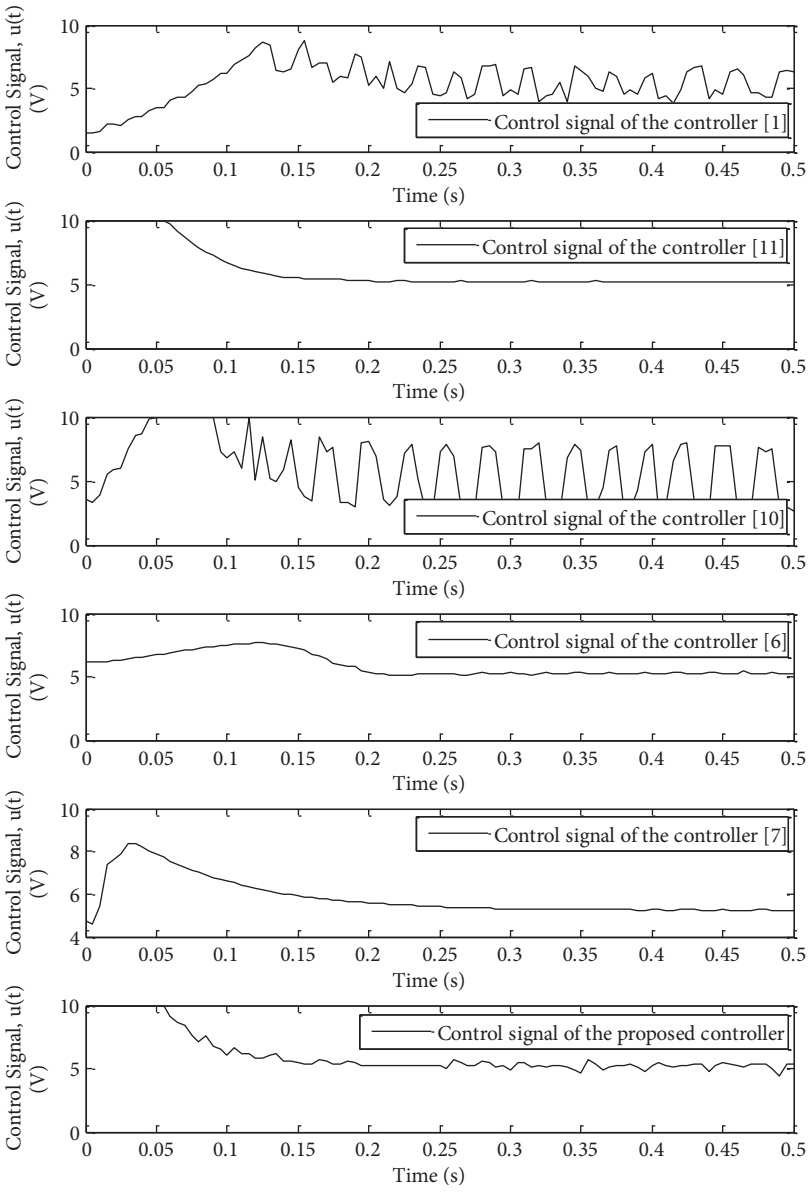

Figure 9. Control signals of the evaluated controllers.

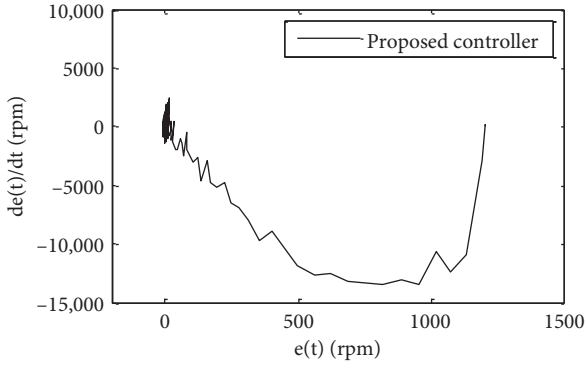

Figure 10. Motion of system trajectories.

Table 5. Results of performance indices.

Shaft speed	Conventional sliding-mode controllers	IAE	ISCI	ISE	ITAE
600 rpm	Controller [1]	0.5218	27.042	0.5442	0.3410
	Controller [11]	0.3062	45.509	0.1978	0.2299
	Controller [10]	0.3209	39.253	0.2332	0.3060
	Controller [6]	0.2590	26.622	0.2719	0.0856
	Controller [7]	0.5793	23.647	0.3697	0.5470
	Proposed controller	1.1588	20.711	0.6750	1.5007
1200 rpm	Controller [1]	0.7892	85.225	2.2854	0.2465
	Controller [11]	0.3197	87.354	0.8959	0.0542
	Controller [10]	0.4876	100.426	1.2578	0.1989
	Controller [6]	0.4591	87.259	1.3622	0.0643
	Controller [7]	0.5241	85.834	1.2382	0.1791
	Proposed controller	0.3475	87.938	0.9025	0.0810
1800 rpm	Controller [1]	1.7385	173.527	8.5133	0.5340
	Controller [11]	2.7080	145.040	4.3618	3.3382
	Controller [10]	0.9330	189.464	3.7249	0.3298
	Controller [6]	0.8954	181.861	3.5464	0.1491
	Controller [7]	1.2029	184.926	3.3584	0.8298
	Proposed controller	0.7536	181.280	2.8223	0.2185

recovered the applied load with a small steady-state error. On the other hand, more steady-state error at the output was observed in the response of the controllers in [1,11].

The tracking performances of the controllers were also investigated by applying a square wave command trajectory that corresponds to 1200 $\pm$ 100 rpm shaft speed as illustrated in Figure 12. Small magnitude of steady-state error was observed at the output when the controller in [11] was used. The maximum settling time was measured when using the controller in [1]. However, the remaining controllers in [6,7,10] and the proposed one showed better tracking performance. The proposed controller provided smoother output than the other controllers [6,7,10].

In the proposed controller, the magnitude of the adaptive parameter of the sliding function, $\beta\left(r(t), t_s\right)$, is proportional to t_s and λ. Thus, the closed-loop experiments at 1200 rpm shaft speed were performed to investigate the system responses with respect to different sampling periods using appropriate λ. The time-domain specifications of the system responses are tabulated in Table 6. The tracking accuracy was greatly

Table 6. Time-domain step response specifications of the proposed controller with respect to different sampling periods.

Sample time t (ms)	λ	$\beta\left(r(t), t_s\right)$	Rise time (ms)	Settling time (ms)	Delay time (ms)	Output speed deviation ($\pm$rpm)
2	6	0.1330	71.5	117	54	7
3	7	0.1716	106.0	156	56	8
4	11	0.4190	95	142	55	8
6	14	0.7984	99	149	69	7
8	14	1.0667	113	144	101	9
10	11	1.1429	123	160	81	8

preserved although different sampling periods were selected. The parameter λ was the only independent parameter tuned by the user easily and the switching control parameters were unchanged.

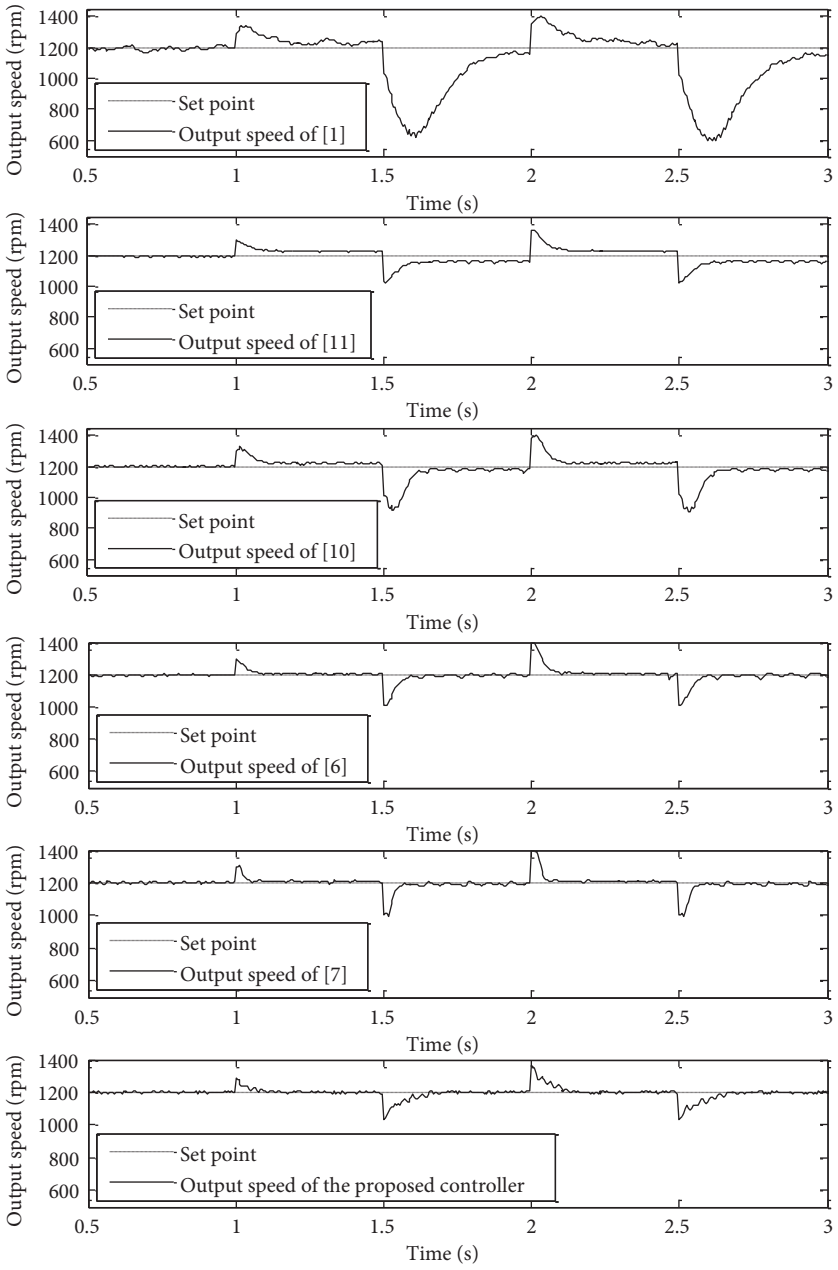

Figure 11. Output speed of the controllers to ± 100 rpm external load disturbance.

5. Conclusion

In this paper, a new approach to adaptive sliding-mode controllers has been proposed. The simplification was taken into account when considering the design of the proposed controller so that the adaptive parameters were obtained from the known parameters of the system. In the proposed controller, the transient state of the output was improved by the switching control gain bounded with the magnitude of the tracking error. Such

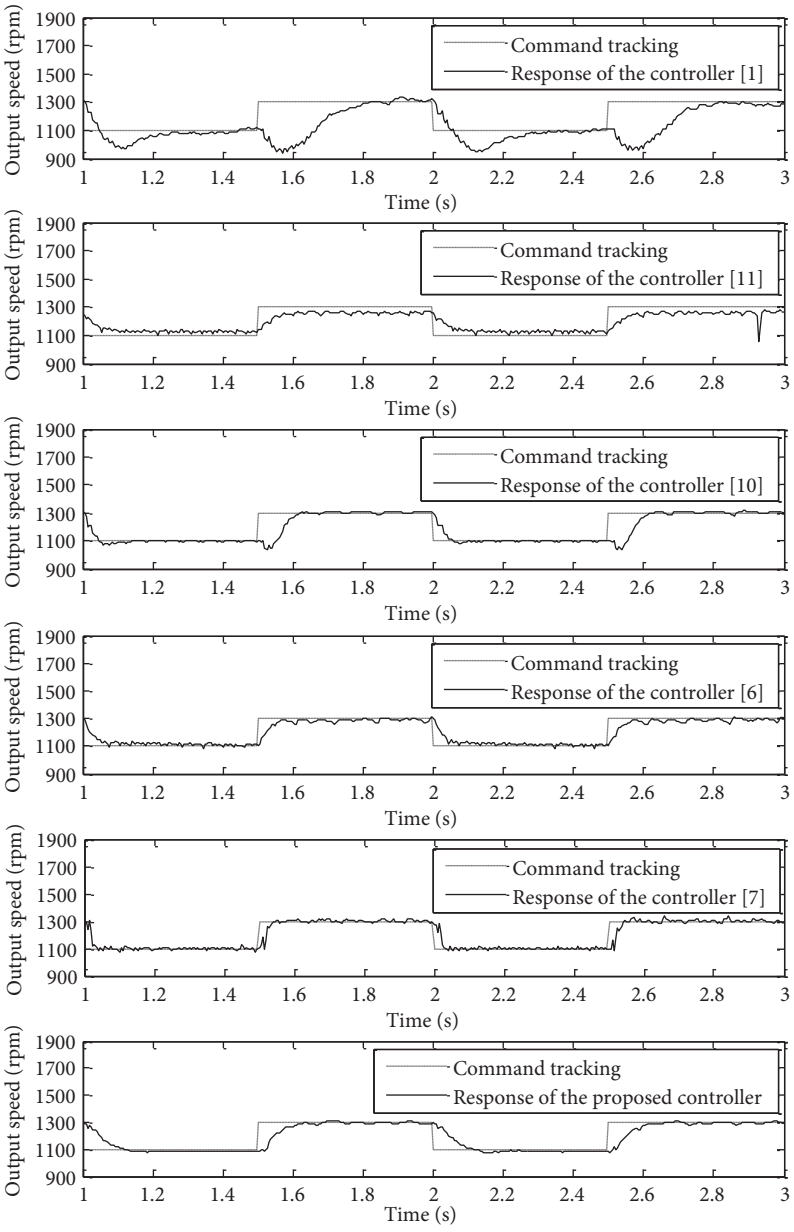

Figure 12. Command tracking responses of the controllers.

an approach also prevented the actuator from chattering in the steady state. Another improvement can be seen in the sliding function definition. A new parameter was included to the sliding function that reduces the variation of the sliding function significantly. The performance of the controller was significantly increased when using different sampling periods. The variation and magnitude of the tracking error were reduced as compared to the other controllers proposed in the literature. The graphical presentations and statistical results verified that the proposed controller is a good candidate and an alternative to the other controllers in the literature to control uncertain real systems, particularly regarding the number of independent gains and chattering level on the control input.

References

[1] Utkin VI. Variable structure systems with sliding modes. IEEE T Automat Contr 1977; 22: 212–222.

[2] Lee H, Utkin VI. Chattering suppression methods in sliding mode control systems. Annu Rev Contr 2007; 31: 179–188.

[3] Lee H, Utkin VI, Malinin A. Chattering reduction using multiphase sliding mode control. Int J Control 2009; 82: 1720–1737.

[4] Monsees G, Scherpen JMA. Adaptive switching gain for a discrete-time sliding mode controller. Int J Control 2002; 75: 242–251.

[5] Husain AR, Ahmad MN, Yatim AHH. Chattering-free sliding mode control for an active magnetic bearing system. Int J Aer Mech 2008; 2: 48–54.

[6] Kaya İ. Sliding mode control of stable processes. Ind Eng Chem Res 2007; 46: 571–578.

[7] Eker İ, Akınal ŞA. Sliding mode control with integral augmented sliding surface: design and experimental application to an electromechanical system. Electr Eng 2008; 90: 189–197.

[8] Tai NT, Ahn KK. A RBF neural network sliding mode control for SMA actuator. Int J Control Aut 2010; 8: 1296–1305.

[9] Levant A. Chattering analysis. IEEE T Automat Contr 2010; 55: 1380–1389.

[10] Eker İ. Sliding mode control with PID sliding surface and experimental application to an electromechanical plant. ISA T 2006; 45: 109–118.

[11] Camacho O, Smith CA. Sliding mode control: an approach to regulate nonlinear chemical processes. ISA T 2000; 39: 205–218.

[12] Tseng ML, Chen MS. Chattering reduction of sliding mode control by low-pass filtering the control signal. Asian J Control 2010; 12: 292–298.

[13] Camacho O, Smith C, Moreno W. Development of an internal model sliding mode controller. Ind Eng Chem Res 2003; 42: 568–573.

[14] Kaynak O, Erbatur K, Ertuğrul M. The fusion of computationally intelligent methodologies and sliding mode control – a survey. IEEE T Ind Electron 2001; 48: 4–17.

[15] Xinghou Y, Kaynak O. Sliding-mode control with soft computing: a survey. IEEE T Ind Electron 2009; 56: 3275–3285.

[16] Zhao F, Utkin VI. Adaptive simulation and control of variable-structure control systems in sliding regimes. Automatica 1996; 32: 1037–1042.

[17] Guo L, Hung JY, Nelms RM. Comparative evaluation of sliding mode fuzzy controller and PID controller for a boost converter. Electr Pow Syst Res 2011; 81: 99–106.

[18] Roopaei M, Jahromi MZ. Chattering-free fuzzy sliding mode control in MIMO uncertain systems. Nonlinear Anal-Theor 2009; 71: 4430–4437.

[19] Mondal S, Mahanta C. Chattering free adaptive multivariable sliding mode controller for systems with matched and mismatched uncertainty. ISA T 2013; 52: 335–341.

[20] Mohseni SA, Tan AH. Optimization of neural networks using variable structure systems. IEEE T Syst Man Cy B 2012; 42: 1645–1653.

[21] Plastan F, Shtessel Y, Bregeault V, Poznyak A. New methodologies for adaptive sliding mode control. Int J Control 2010; 83: 1907–1919.

[22] Furat M, Eker İ. Computer-aided experimental modeling of a real system using graphical analysis of a step response data. Comput Appl Eng Educ 2014: 22: 571–582.

[23] Seborg DE, Edgar TF, Mellichamp DA. Process Dynamics and Control. New York, NY, USA: Wiley, 1989.

[24] Hsiao MY, Li THS, Lee JZ, Chao CH, Tsai SH. Design of interval type-2 fuzzy sliding-mode controller. Inform Sciences 2008; 178: 1696–1716.